

Boundary-driven phase transitions in open two-species driven systems with an umbilic point

Vladislav Popkov^{1,2}

¹ *Max Planck Institute for Complex Systems,*

Nöthnitzer Straße 38, 01187 Dresden, Germany and

² *Dipartimento di Fisica e Astronomia, Università di Firenze,*

via G. Sansone 1, 50019 Sesto Fiorentino, Italy

(Dated: February 26, 2018)

Different phases in open driven systems are governed by either shocks or rarefaction waves. A presence of an isolated umbilic point in bidirectional systems of interacting particles stabilizes an unusual large scale excitation, an umbilic shock (U-shock). We show that in open systems the U-shock governs a large portion of phase space, and drives a new discontinuous transition between the two rarefaction-controlled phases. This is in contrast with strictly hyperbolic case where such a transition is always continuous. Also, we describe another robust phase which takes place of the phase governed by the U-shock, if the umbilic point is not isolated.

I. INTRODUCTION

Many intrinsically nonequilibrium phenomena can be observed already in simplest systems of driven diffusing particles [1, 2], which are paradigmatic models of systems far from equilibrium and find a wide range of applications in biological, social and physical contexts [3–5]. Driving forces due to bulk fields or boundary gradients lead to steady state currents that invalidate the condition of detailed balance and give rise to remarkable features which have no equilibrium counterparts, such as boundary driven phase transitions, spontaneous symmetry breaking and hysteresis in one spatial dimension. Models with two or more conserved species of particles exhibit particularly rich behaviour [6].

The evolution of driven systems on large spatio-temporal scales is governed by two fundamental types of excitations: shocks, which carry discontinuities, and rarefaction waves, which are continuous self-similar solutions of the hydrodynamic limit equations [7]. Various properties of the fundamental excitations like stability, speed and morphology are determined by a scalar or vector function which relates steady macroscopic currents to average particle densities, the so-called current density relation. The topology of the current-density function such as the number of extrema and saddle points determines qualitative features of the large scale dynamics and in particular the number and character of the different stationary phases and phase transitions that one can observe in the underlying microscopic model [8–10]. In this way microscopic details of local par-

ticle interactions are largely irrelevant as long as they produce a certain type of a current density relation.

It was noted [11] that bidirectional particle systems, in which bulk hopping rates of oppositely moving interacting species possess the left-right symmetry, have a special property: their current-density function has an umbilic point. A generic umbilic point is a point on a current-density surface where the two characteristic velocities coincide, which breaks the usual assumption of strict hyperbolicity [12]. For bidirectional systems with left-right symmetry, both characteristic velocities vanish at the umbilic point which can be isolated or not, depending on a strength of an interaction between the species. An isolated umbilic point, in an open system under maximal feeding regime (a regime where particles enter and exit the system freely) stabilize a large scale excitation reminiscent of a shock wave, but which should be unstable according to usual shock stability criteria [13],[14]. The new excitation was called an umbilic shock, or a U-shock, and studied on microscopic scale [11].

In present article we determine a domain on the phase diagram which is controlled by a U-shock, and identify a boundary driven phase transition that it governs. Boundary-driven phase transitions in driven systems, which are caused by adiabatical changes of boundary conditions have no equilibrium counterparts [15],[8],[16]. They may be continuous or discontinuous, depending on whether the order parameter changes across the transition in a continuous or discontinuous way. We show that a U-shock governs a discontinuous phase transition from one rarefaction-wave controlled state to another. Such a transition in a usually considered strictly hyperbolic systems (without an umbilic point) is always continuous [10]. If the umbilic point is not isolated, the U-shock is no longer stable, but on its place we find another robust phase, a homogeneous bulk state with densities matching the umbilic point. This state, which we call the umbilic state, has the same stability domain as the U-shock phase. A boundary driven phase transition leading to the umbilic state occurs via a continuous transition. We expect our results to be generally valid for any system with an umbilic point; however for definiteness we consider a model for which the current-density relation is known exactly.

The plan of the paper is the following: In Sec. II we introduce our model. In Sec. III we discuss splitting of the physical region according to signs of characteristic velocities, and review the U-shock and the umbilic phase. In Sec.IV we describe phase transitions from and to the phases controlled by umbilic point, along a trajectory, where boundary rates are changed adiabatically. There, we also describe the domain of stability of the umbilic point- controlled phases. We finish with conclusions and perspectives. Appendices contain necessary technical details.

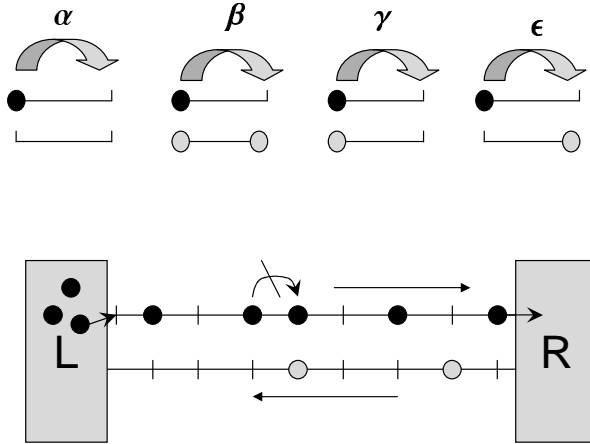


Figure 1: Bidirectional two-chain model. For solvability, the rates must satisfy $\alpha = \beta = \varepsilon = 1$, $\gamma = e^\nu$ where ν is the interchain interaction constant [19]. Coupling to boundary reservoirs is indicated by boxes marked L (the left reservoir) and R (the right reservoir).

II. THE BIDIRECTIONAL MODEL WITH BOUNDARY RESERVOIRS

Our model describes particles with repulsive hard-core interaction which hop unidirectionally along two chains of N sites: One chain for right-hopping particles and another chain for left-hopping particles. At each instant of time the system is fully described by occupation numbers $n_k \in \{0, 1\}$ (for the right movers) and $m_k \in \{0, 1\}$ (for the left-movers). A right-moving particle at site k can hop to its neighbouring site $k + 1$ provided it is empty, with a rate that depends on the occupancies at sites $k, k + 1$ on the adjacent chain, see Fig.1. E.g. a particle hops with rate β if the adjacent sites are both occupied, etc. For clarity of presentation and analytic simplification we shall keep only one rate $\gamma = e^\nu$ different from others, setting all remaining rates to 1,

$$\alpha = \beta = \varepsilon = 1, \quad \gamma = e^\nu \quad (1)$$

Then the parameter

$$Q = \gamma - 1 \quad (2)$$

which ranges from -1 to ∞ , measures the interaction strength between the left- and right-moving species. For $Q = 0$ the model reduces to two independently running totally asymmetric exclusion processes [17],[18].

The bulk dynamics of particles (see Fig.1) is complemented with boundary conditions: we consider open boundaries where at the left end of the chain a right mover can enter the chain and it can leave it at the right end. Left movers are hopping to the left with the same dynamic rules. The boundary hopping rates are chosen so as to correspond to particle reservoirs with effective

densities of right- and left movers u_L, v_L at the left boundary, and u_R, v_R at the right boundary, see Appendix A. Note that generically $u_L \neq v_L, u_R \neq v_R$, so that while the bulk dynamics is left-right symmetric, the entrance and exit rates for different species are not. After a certain transition period, the system will approach a stationary state, characteristics of which (the average flux, the density profile, the correlations) do not depend on time.

For our dynamical Monte-Carlo simulation we choose the following random sequential update procedure. For a chain of length N , i.e. a system of $2N$ sites (numbered $i = 1, 2, \dots, N$ for right movers and $i = N + 1, N + 2, \dots, 2N$ for left movers) one Monte-Carlo step consists of $2N + 2$ uniform drawings of an integer random number w in the range $0 \leq w \leq 2N + 1$. If $0 \leq w \leq N$, the configuration of right movers is updated. If $w = 0$, and the left boundary site $i = 1$ is empty, we fill it with a particle with a rate parametrized by boundary reservoir densities u_L, v_L , see Appendix A. If $w = N$ and the respective site contains a particle, we remove it with a rate parametrized by boundary reservoir densities u_R, v_R , see Appendix A. For intermediate $0 < w < N$, if site w contains a particle, a hopping is performed on the right neighbouring site with given rates (1), provided it was empty. The update of the left movers is done analogously. We start from an empty lattice and after a transient time we measure site occupancies n_k, m_k , and take averages over many Monte Carlo steps and many histories. We choose a system size up to $L = 500$ sites in each chain. The transient time for $L = 500$ is 10^5 Monte Carlo steps, and averaging over up to 10 histories is done.

In contrast to our study [11] which was focused on microscopic features, here we focus on large-scale hydrodynamic behaviour of an open system with an umbilic point. To this end, we also use an improved meanfield approach, described in Appendix B. Results obtained by the stochastic approach and the meanfield approach agree well, both for system dynamics and for steady state global averages, due to product-measure steady state property on a ring (A1).

III. SPLITTING OF PHYSICAL REGIONS ACCORDING TO SIGNS OF CHARACTERISTIC VELOCITIES

Characteristic velocities $c_1(u, v)$ and $c_2(u, v)$ are velocities with which infinitesimal perturbations are propagating, on top of a stationary homogeneous background with average densities of right- and left-moving particles u and v . As such, they play a fundamental role in the stability of large scale excitations [19].

The characteristic velocities can be obtained by solving an eigenvalue problem for a flux Jacobian

$(Dj)\Psi_k = c_k\Psi_k$ where

$$(Dj) = \begin{pmatrix} \frac{\partial j_1}{\partial u} & \frac{\partial j_1}{\partial v} \\ \frac{\partial j_2}{\partial u} & \frac{\partial j_2}{\partial v} \end{pmatrix}. \quad (3)$$

For our model (1) the particle currents j_1 and j_2 can be obtained analytically, see [11] for details, and are given by

$$j_1(u, v) = u(1 - u) + Q\Omega_{11}(u, v)\Omega_{00}(u, v) \quad (4)$$

$$j_2(u, v) = -j_1(v, u) = -v(1 - v) - Q\Omega_{11}(v, u)\Omega_{00}(v, u), \quad (5)$$

where Ω_{11} and Ω_{00} are stationary probabilities to have two adjacent particles and two adjacent holes,

$$\Omega_{11} = \frac{(u + v - 1)Q - 1 + \sqrt{((u + v - 1)Q - 1)^2 + 4Quv}}{2Q} \quad (6)$$

$$\Omega_{00} = 1 - u - v + \Omega_{11}.$$

Due to the hardcore exclusion, the average densities of the right and left-moving particles may only take values between 0 and 1. The whole physical region of $0 \leq u, v \leq 1$ is then splitted into regions $G_{\sigma\tau}$ with different signs of characteristic velocities, which is illustrated in Fig.2. Subscripts σ, τ denote signs the characteristic speeds c_1 and c_2 , i.e. $\sigma = 0, +, -$ correspond to $c_1 = 0, c_1 > 0, c_1 < 0$, and similarly for τ . E.g. we name by G_{-+} a region on $u - v$ plane where $c_1(u, v) < 0$ and $c_2(u, v) > 0$. Note that the characteristic speeds are numerated in increasing order, $c_1 < c_2$.

As we can see in Fig.2, the splitting contains a special point, an umbilic point, $u^* = v^* = \frac{1}{2}$, where characteristic velocities both vanish, $c_1(u^*, v^*) = c_2(u^*, v^*) = 0$, for any value of Q , as can be straightforwardly verified from (4),(5). For $Q > Q_{crit} = -\frac{3}{4}$, the umbilic point is a crossing point of the curves $c_1(u, v) = 0$ and $c_2(u, v) = 0$, see Fig.2(a). The respective current-density surfaces $j_k(u, v, Q)$ have a regular convex topology. For $Q < Q_{crit}$, current-density surfaces $j_k(u, v, Q)$ develop a saddle point, and the umbilic point becomes an isolated point, see Fig.2(b).

Characteristic speeds determine stability of large scale excitations in our system, described on the macroscopic scale by a system of conservation laws for coarse-grained densities $u(x, t), v(x, t)$

$$\partial_t u + \partial_x j_1(u, v) = 0 \quad (7)$$

$$\partial_t v + \partial_x j_2(u, v) = 0,$$

j_1 and j_2 being steady particle currents [20], complemented with boundary conditions

$$u(0, t) = u_L; \quad u(1, t) = u_R,$$

$$v(0, t) = v_L; \quad v(1, t) = v_R.$$

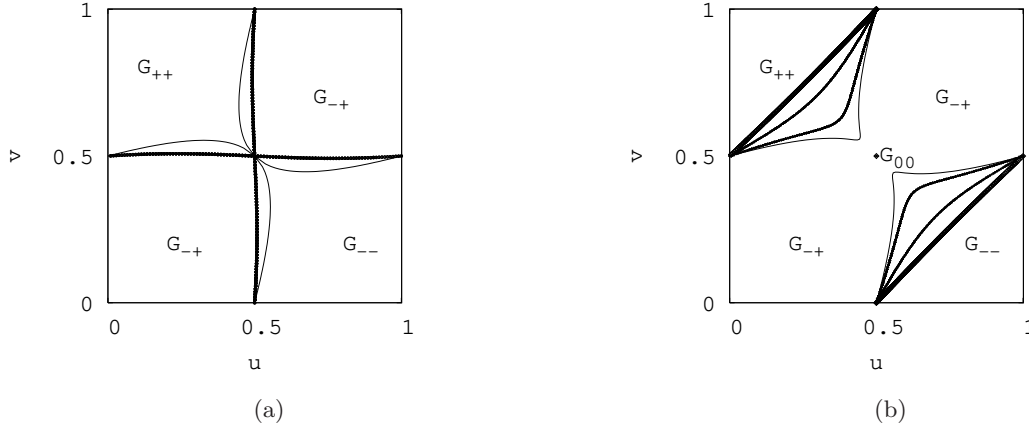


Figure 2: Splitting of the physical region into domains G_{++}, G_{--}, G_{-+} according to signs of characteristic velocities, for different Q . Boundaries between the domains, on which one characteristic velocity vanishes $c_i(u, v) = 0$, are marked by lines. Point $u = v = 1/2$ is an umbilic point where $c_1 = c_2 = 0$ for any value of Q . (**Panel (a)**): $Q \geq Q_{crit}$. Thick and thin lines stand respectively for $Q = -0.5, -0.75$. Umbilic point is situated at the crossing of two curves. **Panel (b)**: $Q \leq Q_{crit}$. Lines, in order of increasing thickness, correspond to $Q = -0.76, -0.8, -0.9, -0.99$. Umbilic point, marked by G_{00} , is an isolated point.

A commonly made assumption about the flux functions j_1, j_2 , called strict hyperbolicity, reads: the characteristic speeds are different $c_1(u, v) \neq c_2(u, v)$ for all u, v . Strictly hyperbolic systems have only two types of fundamental solutions: shocks and rarefaction waves [14]. Presence of an umbilic point ruins strict hyperbolicity and results in appearance of novel excitations listed below.

An isolated umbilic point in our system (for $Q < -3/4$) was related to an existence of a large-scale excitation, called U-shock: it is microscopically sharp like a shock but according to usual stability criteria it should be unstable [11]. The U-shock interface, see Fig.3(a), is connecting two rarefaction waves [21]. If the umbilic point is not isolated (for $Q \geq -3/4$), the U-shock reduces to a bulk homogeneous state with $c_1 = c_2 = 0$, meaning that it has densities $u^* = v^* = 1/2$, matching the umbilic point. We call this state an umbilic state. Both U-shock and umbilic state profiles have a property of being left-right symmetric, while the boundary conditions, generically, are not. In the next section we describe the domain on the phase diagram, occupied by umbilic point-related phases, and the respective phase transitions.

IV. BOUNDARY-DRIVEN PHASE TRANSITIONS CONTROLLED BY UMBILIC POINT

The splitting of the physical region, done in the previous section, allows to study a phase diagram of an open system, and transitions between those, in a systematic manner. A transition from one

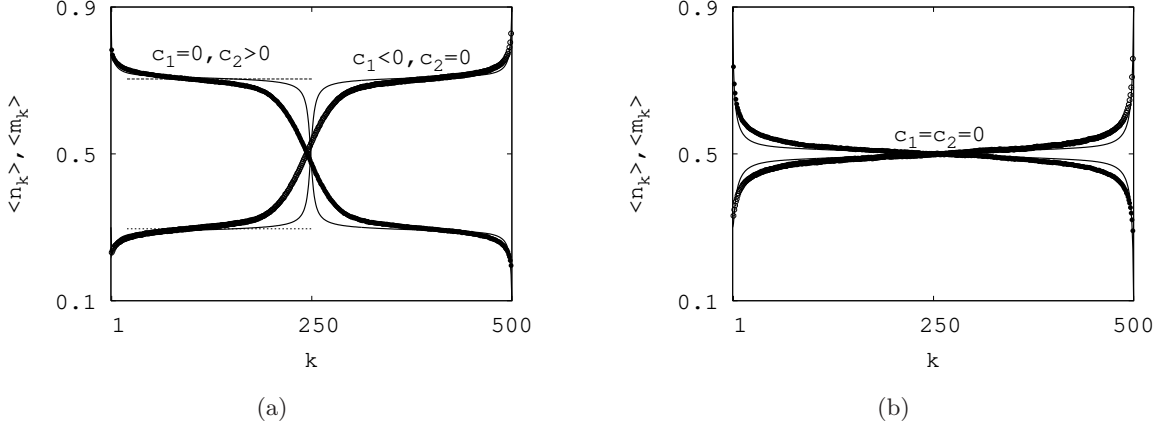


Figure 3: Average density profiles in phases controlled by umbilic point in a bidirectional model Fig.1, for $Q = -0.9 < Q_{crit}$ (**Panel (a)**) and $Q = -0.5 > Q_{crit}$ (**Panel (b)**). Symbols are data points obtained from Monte Carlo simulations while lines are given by numerical solution of hydrodynamic equations (B1). Values of the characteristic velocities are indicated on top of density profiles. Parameters: $N = 500$, $(u_L, v_L) = (0.9, 0.3)$, $(u_R, v_R) = (0.1, 0.9)$. Note that bulk profiles are left-right symmetric while the boundary rates are not. Broken lines on Panel (a) indicate theoretically predicted bulk values, the U-shock amplitude being equal to 2Δ where Δ is given by (9). Both umbilic point-controlled phases are stable, if $(u_L, v_L) \in G_{--}$ and $(u_R, v_R) \in G_{++}$, see also Tables I,II

phase to another in an open system with fixed bulk rates happens by a gradual adiabatic change of the boundary rates, which amounts to a respective adiabatic change of boundary densities u_L, v_L, u_R, v_R . Such a gradual change defines a path, or trajectory in the 4-dimensional space $\Gamma(s) \equiv \{u_L(s), v_L(s), u_R(s), v_R(s)\}$, parametrized by a running variable s . Choosing the average particle densities u, v in the steady state as an order parameter, we study a correspondence $\Gamma(s) \rightarrow (u(s), v(s))$, which shows singular behaviour at the critical points s_{crit} along a path. Across a critical point a transition between two neighbouring phases takes place, which, see [10] is always governed by a large scale excitation- either a shock or a rarefaction wave, depending on how boundary changes are performed. To specify, denote the number of positive characteristic velocities in the left (right) boundary reservoir as $\#_L$ ($\#_R$), which can then take integer values $\#_R, \#_L = 0, 1, 2$. A transition from one phase to another is governed by a rarefaction wave if $\#_L(s) \leq \#_R(s)$ for all s . A straightforward example of a path $\Gamma(s)$ satisfying the requirement $\#_L(s) \leq \#_R(s)$, is a Ph2 path described by steps I,II,III below, see also first two columns of Table I. In a strictly hyperbolic system a mapping $\Gamma(s) \rightarrow (u(s), v(s))$ along a Ph2 path is continuous [10].

An isolated umbilic point, present in our model for large interlane interactions $Q < -3/4$, stabilizes a sharp interface connecting two rarefaction waves, a so-called a U-shock [11]. Below we demonstrate that the U-shock makes possible a discontinuous change $\Gamma(s) \rightarrow (u(s), v(s))$ along a

Ph2 path in a system with an isolated umbilic point.

In order to clarify the influence of a U-shock on the phase diagram we consider a Ph2 path [22] from a steady state G_{++} to a steady state G_{--} , in presence and in absence of an isolated umbilic point. Let us denote by $0 \leq s \leq 1$ a variable parametrizing the adiabatic Ph2 path, and by $u_L(s), v_L(s), u_R(s), v_R(s)$ the respective densities of boundary reservoirs. As in [10], we shall vary the boundary densities along the Ph2 path in the following way:

I. Initial point $s = 0$ and final point $s = 1$ corresponds to fully-matching left and right boundary reservoirs. $u_L(0) = u_R(0) = u^{initial}, v_L(0) = v_R(0) = v^{initial}$, where $c_1(u^{initial}, v^{initial}) > 0, c_2(u^{initial}, v^{initial}) > 0$. Analogously for $u_L(1) = u_R(1) = u^{final}, v_L(1) = v_R(1) = v^{final}$, where $c_1(u^{final}, v^{final}) < 0, c_2(u^{final}, v^{final}) < 0$.

II. For $0 \leq s \leq \frac{1}{2}$, left boundary densities $u_L(s), v_L(s)$ are changing smoothly from $u^{initial}, v^{initial}$ to u^{final}, v^{final} at $s = 1/2$. The right boundary densities remain the same, $u_R(s \leq 1/2) = u^{initial}, v_R(s \leq 1/2) = v^{initial}$.

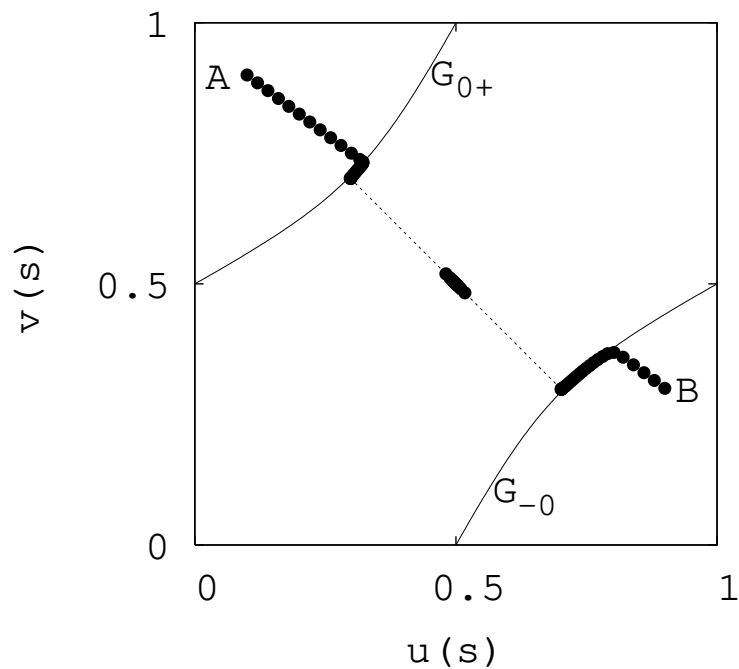
III. For $\frac{1}{2} \leq s \leq 1$, the right boundary densities $u_R(s), v_R(s)$ are changing smoothly from $u^{initial}, v^{initial}$ at $s = \frac{1}{2}$ to u^{final}, v^{final} at $s = 1$. The left boundary densities remain the same, $u_L(s \geq 1/2) = u^{final}, v_L(s \geq 1/2) = v^{final}$.

As argued in [10], all along such a path the steady state is controlled by rarefaction waves. In absence of an umbilic point, rarefaction waves do not have any discontinuities [14],[13], and therefore the stationary densities along the path $u(s), v(s)$ are expected to change continuously with s .

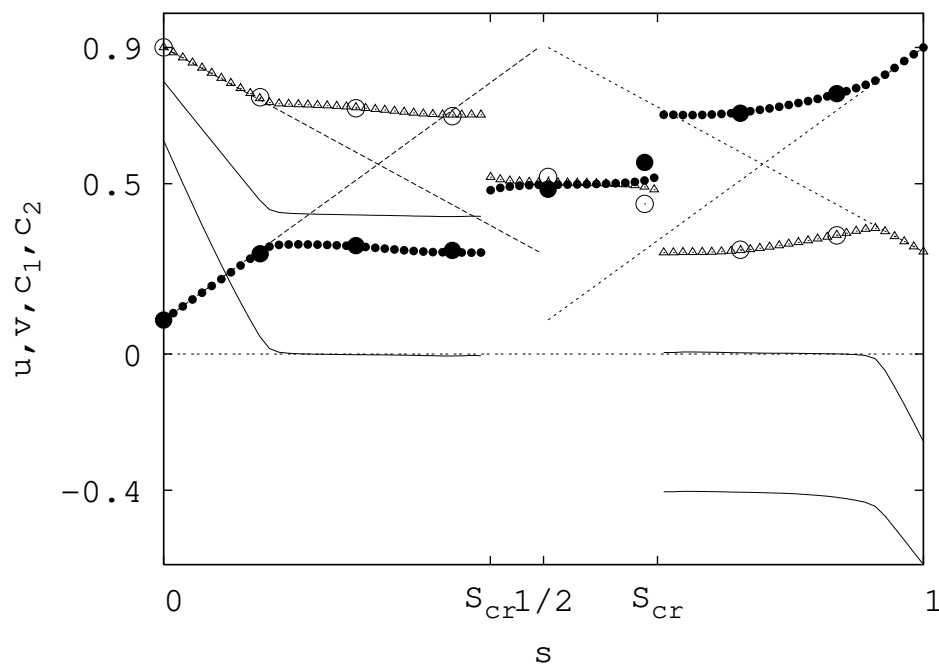
In the following we demonstrate that an isolated umbilic point provokes two discontinuous jumps of $u(s), v(s)$, and locate the critical point. The jumps are due to a motion of the U-shock between the boundaries which become biased at the transition point.

We choose the initial and the final state to be $(u^{initial}, v^{initial}) = (0.1, 0.9)$ and $(u^{final}, v^{final}) = (0.9, 0.3)$, and change the boundary densities for intermediate s by linear interpolation, i.e. $u_L(s) = u^{initial} + 2s(u^{final} - u^{initial}), v_L(s) = v^{initial} + 2s(v^{final} - v^{initial})$ for $0 \leq s \leq 1/2$, and similarly for $s \geq 1/2$. After that we perform an adiabatic Ph2 path for a system with an isolated umbilic point $Q = -0.9 < Q_{crit}$, and non-isolated umbilic point $Q = -0.5 < Q_{crit}$. For both values of Q , $(u^{initial}, v^{initial}) \in G_{++}$ and $(u^{final}, v^{final}) \in G_{--}$. We present the results in Figs. 4,5.

Case 1. Isolated umbilic point. An isolated umbilic point appears above the critical interaction amplitude, $Q < -\frac{3}{4}$. In this case, Fig. 4(a), we see a discontinuous change in average stationary densities $u(s)$ and $v(s)$ at two points s_{crit}^1, s_{crit}^2 . As already stressed, this discontinuous phase transition is impossible in a strictly hyperbolic system. A closer examination reveals the mechanism of the new transition. Firstly, we notice that the steady state of a system is a U-shock

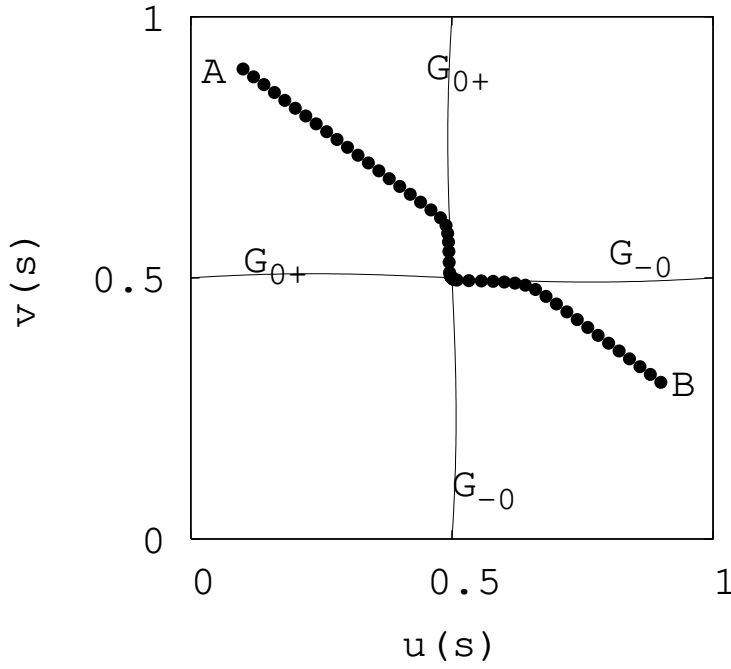


(a)

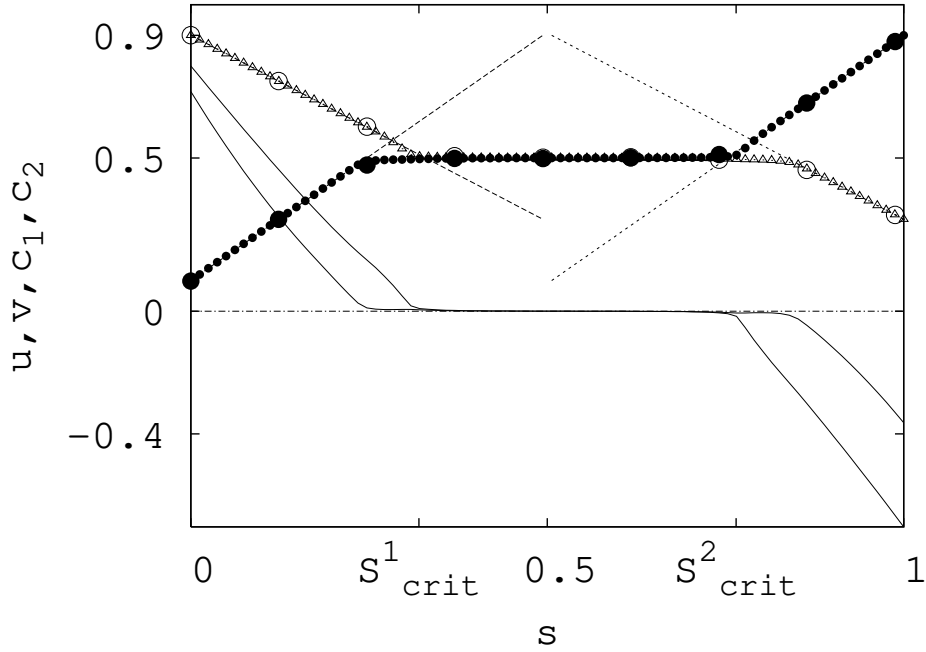


(b)

Figure 4: **Panel (a)**: Location of stationary bulk densities $u(s), v(s)$ along the Ph2 path on a $u-v$ plane, in case of isolated umbilic point. Points A and B mark initial and final point of the path, respectively. Curves marked G_{0+} and G_{-0} denote location of points with $c_1(u, v) = 0$ and $c_2(u, v) = 0$, respectively. Broken line mark a discontinuous transition to the U-shock phase. Spreading of the points in the middle is due to finite size-effects. **Panel (b)**: Stationary bulk densities $u(s), v(s)$ of the right movers (small circles) and of the left movers (triangles) along the Ph2 path. Broken lines denote the dependence of $(u_L(s), v_L(s))$ for $s < 1/2$ and $(u_R(s), v_R(s))$ for $s > 1/2$. Thin lines denote $c_k(u, v)$. Critical points s_{cr} mark discontinuous transitions to the U-shock phase. Most data are obtained by numerical integration of the meanfield equations. Large circles



(a)



(b)

Figure 5: **Panel (a)**: Location of stationary bulk densities $u(s), v(s)$ along the Ph2 path on a $u - v$ plane, for $Q = -0.5$. Points A and B mark initial and final point of the path, respectively. Curves marked G_{0+} and G_{-0} denote location of points with $c_1(u, v) = 0$ and $c_2(u, v) = 0$, respectively. **Panel (b)**: Stationary bulk densities $u(s), v(s)$ of the right movers (circles) and of the left movers (triangles) along the Ph2 path. Broken lines denote the dependence of $(u_L(s), v_L(s))$ for $s < 1/2$ and $(u_R(s), v_R(s))$ for $s > 1/2$. Thin lines denote $c_k(u, v)$. Critical points s^1_{crit} and s^2_{crit} mark transitions to the umbilic phase. Results are obtained by numerical integration of the meanfield equations. Large circles on Panel(b) mark steady state densities obtained from Monte-Carlo simulations. Parameters: $Q = -0.5$. $N = 200$.

if

$$(u_L, v_L) \in G_{++} \quad \text{and} \quad (u_R, v_R) \in G_{--}, \quad (8)$$

which corresponds to a segment $s \in [s_{crit}^1, s_{crit}^2]$ of the adiabatic Ph2 trajectory. The U-shock is an interface between the two rarefaction waves. The average bulk densities to the left and to the right from the interface depend only on Q and are given by $u, v = \frac{1}{2} \pm \Delta$, where

$$\Delta = \frac{1}{4} \sqrt{3Q^{-1} + 4}. \quad (9)$$

The above values of u, v correspond to maxima of the current density relation $j(u, v, Q)$, which develops a saddle point for $Q < -3/4$, see Fig.6. Steady-state currents of both species have the same amplitude, $j_1^U = -j_2^U = 1/(8|Q|)$.

As long as the conditions (8) are satisfied, the bulk densities, and consequently the steady currents, do not depend on boundary densities. The boundary densities affect only the respective boundary layers, interpolating between the bulk and the boundary, on a microscopic scale. The interface position fluctuates with time around the center of the lattice.

Now consider a left vicinity of a critical point $s = s_{crit}^1 - \varepsilon$, where $0 < \varepsilon \ll 1$. Once $\varepsilon > 0$, the U-shock is biased to the left, and gets pinned to the left boundary. The resulting steady state is homogeneous with the densities $u = \frac{1}{2} - \Delta, v = \frac{1}{2} + \Delta$. With ε increasing, $(u(s), v(s))$ follows the curve G_{+0} .

Analogously, at the other side of the U-shock phase, in the right vicinity of another critical point $s = s_{crit}^2 + \varepsilon$, the U-shock is biased to the right. This results in a homogeneous steady state with the densities $u = \frac{1}{2} + \Delta, v = \frac{1}{2} - \Delta$, where Δ is given by (9). As s increases, the point $(u(s), v(s))$ follows the curve G_{0-} . Depinning from the curve G_{0-} occurs when both $(u_L, v_L) \in G_{++}$ and $(u_R, v_R) \in G_{++}$.

Steady states and corresponding reservoir densities are listed in order of their temporal appearance along the adiabatic trajectory on Table I. As one can see, steady states are straightforwardly connected to the phase space splitting in subregions $G_{\alpha\beta}$ with different signs of characteristic velocities.

It is instructive to compare the discontinuous U-shock-governed phase transition described above to a usual discontinuous phase transition in driven systems governed by a standard Lax shock [13]. In the latter, the shock changes the sign of a bias at the critical point. Exactly at the critical point, the shock is unbiased, and, due to fluctuations, performs a random walk between the boundaries. On the contrary, in a U-shock –controlled phase transition, the U-shock stays unbiased in the whole segment $[s_{crit}^1, s_{crit}^2]$, defined by (8). For s within this segment, the U-shock position is not

(u_L, v_L) belong to	(u_R, v_R) belong to	Steady state belongs to	Steady state densities
G_{++}	G_{++}	G_{++}	$u = u_L, v = v_L$
G_{-+}	G_{++}	G_{0+}	pinned to G_{0+}
G_{--}	G_{++}	G_{0+}/G_{-0}	U-shock $u = \frac{1}{2} \pm \Delta, v = \frac{1}{2} \mp \Delta$
G_{--}	G_{-+}	G_{-0}	pinned to G_{-0}
G_{--}	G_{--}	G_{--}	$u = u_R, v = v_R$

Table I: Steady states densities $u(s), v(s)$ and corresponding particle densities in boundary reservoirs along a Ph2 path. Δ is given by (9).

(u_L, v_L) belong to	(u_R, v_R) belong to	Steady state belongs to	Steady state densities
G_{--}	G_{++}	G_{00}	umbilic point rarefaction $u = v = \frac{1}{2}$

Table II: Open bidirectional system with a non-isolated umbilic point. Steady states and corresponding boundary reservoir densities along the middle part of a Ph2 path. For remaining path segments, see Table I

performing a random walk between the boundaries, but fluctuates around the middle point as if it was in a potential well.

Case 2. Non-isolated umbilic point. Now, let us push the interaction Q towards the critical point $Q_{crit} = -3/4$. The U-shock amplitude 2Δ becomes smaller and smaller until it disappears at the critical point $\Delta(Q_{crit}) = 0$. The whole U-shock-governed phase above the critical point $Q \geq Q_{crit}$ reduces to a homogeneous phase with densities matching the umbilic point $c_1(u, v) = c_2(u, v) = 0$, see Table II. In this way, the umbilic point defines a robust phase on the phase diagram, which we shall call an umbilic phase or U-phase. The U-phase with $c_1 = c_2 = 0$ appears to be stable whenever $(u_L, v_L) \in G_{--}$ and $(u_R, v_R) \in G_{++}$, see Table II, in the very same domain where a U-shock is stable (8). A pinning-depinning transition from the U-phase is continuous, in contrary to a transition from/to U-shock -governed phase for $Q < Q_{crit}$ discussed earlier, see Fig.5.

Several comments are in order at this point. Firstly, note that the steady state particle currents and bulk density profiles for an umbilic phase and for a U-shock phase are left-right symmetric (so as the bulk hopping rates), in spite of boundary conditions being explicitly not left-right symmetric. Away from the umbilic (or U-shock) phase, a steady state is sensitive to the boundaries and in general is not left-right symmetric. In this way, when entering the respective U-phases, the steady state becomes insensitive to boundaries and regains its bulk symmetry. In absence of umbilic points (i.e. in strictly-hyperbolic systems), steady states are generically boundary-rates dependent.

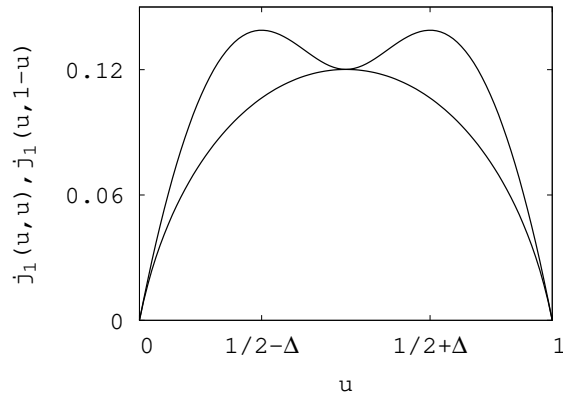


Figure 6: Cuts of the surface $j_1(u, v)$ along the lines $u = v$ (the convex curve) and $u = 1 - v$ (the curve with double maximum), for $Q < Q_{crit}$. Parameters: $Q = -0.9$. Points $u = 1/2 \pm \Delta$ correspond to current maxima, Δ is given by (9). Above the critical point $Q > Q_{crit}$ both cuts are convex.

Secondly, we observe that the total current of both species $j_1 + |j_2|$ along the Ph2 path attains its maximal value just for an umbilic phase and of a U-shock phase. This fact exemplifies a validity of the maximal current principle for bidirectional systems. Indeed, in systems with one driven particle species and open boundaries the maximal current principle asserts in particular that for maximal feeding regime (when both entrance and exit rates are maximal), the stationary current is maximized with respect to an average particle density ρ , $j_{steady} = \max_{\rho \in [0, \rho_{max}]} j(\rho)$. In our model with two species, such a maximal feeding regime is realized when $(u_L, v_L) = (1, 0)$ and $(u_R, v_R) = (1, 0)$, which, consulting the Fig.2 and (8), corresponds to the U-shock or Umbilic phase domain, depending on the value of Q . The respective maximal value of the total current is $j_1 + |j_2| = 2j_1 = (4|Q|)^{-1}$ for U-shock $Q < Q_{crit}$ and $j_1 + |j_2| = 2j_1(u = \frac{1}{2}, v = \frac{1}{2}) = \sqrt{Q+1}/(\sqrt{Q+1}+1)$ for the umbilic phase $Q \geq Q_{crit}$, as can be straightforwardly derived from analytic expressions for the currents.

V. CONCLUSIONS

We conclude that a presence of an umbilic point in the current-density function, isolated or not, gives rise to new types of boundary driven phase transitions. If the umbilic point is an isolated one, one has a discontinuous transition from G_{0+} steady state to the U-shock state G_{0+}/G_{-0} and another discontinuous transition from the U-shock state to G_{-0} state, both transitions governed by a biased motion of a U-shock. In case of non-isolated umbilic point, two continuous (pinning-depinning) transitions $G_{0+} \rightarrow G_{00}$ and $G_{00} \rightarrow G_{-0}$ take place. All these transitions are observable along any Ph2 path, leading from a state with positive characteristics to a steady state with

negative characteristics via adiabatically changing boundary conditions. There is no hysteresis of any kind, so by inversion of the path the sequence of transitions is inverted. The U-shock phase and umbilic phases are robust, and exemplify the validity of a maximal current principle for bidirectional particle models. We identified the domain on the phase diagram occupied by umbilic point related phases (8). Within this domain the system regains its bulk left-right symmetry in spite of the boundary conditions being explicitly not left-right symmetric.

How robust are our results? First of all, the umbilic point with $c_1 = c_2 = 0$ is a general feature of a models with left-right symmetry of hopping rates [11], of which we considered a special example with an exactly known steady state on a ring. We expect qualitatively similar results for general particle systems whether "solvable" or not. In an open system it is only necessary to maintain a stationary maximal flow regime to find out whether the umbilic point is isolated or not. Appearance of a discontinuity in a bulk density profile in the maximal flow regime would indicate that an umbilic point has become isolated. In such a way from a simple single macroscopic observation of a system one can judge on intrinsic differential properties of its current-density function.

Bidirectional models are being widely studied in the literature, in particular, in connection with the intriguing phenomenon of spontaneous symmetry breaking (SSB) [23]-[32]. In most studies however the current-density function is a convex surface. It would be interesting to study SSB in presence of an isolated umbilic point. It is interesting to note that bidirectional models have also an integrability aspect [34], however up to now no example of an integrable system with open nontrivial boundary conditions have been presented.

Acknowledgements

V.P. thanks the IZKS and the University of Bonn for hospitality and acknowledges a partial support by the Alexander von Humboldt foundation, and by the italian MIUR through PRIN 20083C8XFZ initiative.

Appendix A: Boundary rates

Boundary rates for injection and extraction of the particles are chosen so that constant densities of particles are kept on the left and on the right boundary. Steady state of our model with the rates (1) for a system on a ring has a remarkable property: for a configuration C the stationary probability is given by a product measure

$$P_C = Z^{-1} \prod_k e^{-\nu_k m_k}, \quad (\text{A1})$$

where $n_k, m_k = 0, 1$ are particle occupation number on site k on chains 1 and 2, and Z is a normalization. We see that neighbouring pairs of adjacent sites are uncorrelated. This fact allows to express all steady state equal-time expectations in terms of probabilities of a single pair of adjacent sites $\Omega_{n_k m_k}(u, v)$ where u, v is an average density of right and left movers. We have $\Omega_{00} + \Omega_{11} + \Omega_{01} + \Omega_{10} = 1$, $\Omega_{10} + \Omega_{11} = u$, $\Omega_{01} + \Omega_{11} = v$, and $\Omega_{11}(u, v)$ is given by (6). Procedure, completely analogous to that in [33] results in the following definition of the boundary rates: a right-moving particle is injected to a site 1 with rate u_L (with rate $u_L + Q\Omega_{11}(u_L, v_L)$) if an adjacent site is empty (filled). A right-moving particle is extracted from site N with rate $1 - u_R$ (with rate $1 - u_R + Q\Omega_{00}(u_R, v_R)$) if an adjacent site is filled (empty). Analogously, left moving particles are injected at the right boundary with rate v_R (with rate $v_R + Q\Omega_{11}(v_R, u_R)$) if an adjacent site is empty (filled), and extracted at the left boundary with rate $1 - v_L$ (with rate $1 - v_L + Q\Omega_{00}(v_L, v_L)$) if an adjacent site is filled (empty). In case of matching left and right boundaries, $u_L = u_R = u, v_L = v_R = v$, the exact steady state of the system is (A1), independently of system size N .

Appendix B: Meanfield equations

In our meanfield approximation, we neglect correlations between the adjacent pairs of sites, which are also absent in the steady state (A1) but not between the adjacent sites. The equations are obtained by averaging the exact operator equations of motion for occupation number operators \hat{n}_k, \hat{m}_k , which for right-moving particle at site k read

$$\frac{\partial \langle n_k \rangle}{\partial t} = \langle \hat{j}_{k-1, k} \rangle - \langle \hat{j}_{k, k+1} \rangle$$

where $\hat{j}_{k, k+1} = \langle \hat{n}_k(1 - \hat{n}_{k+1}) \rangle + Q \langle \hat{n}_k \hat{m}_k(1 - \hat{n}_{k+1})(1 - \hat{m}_{k+1}) \rangle$. Denoting $\langle \hat{n}_k(t) \rangle = s_k(t)$, $\langle \hat{m}_k(t) \rangle = q_k(t)$, we simplify parts of above expression as $\langle \hat{n}_k(1 - \hat{n}_{k+1}) \rangle \approx \langle \hat{n}_k \rangle \langle 1 - \hat{n}_{k+1} \rangle = s_k(1 - q_{k+1})$ and $\langle \hat{n}_k \hat{m}_k(1 - \hat{n}_{k+1})(1 - \hat{m}_{k+1}) \rangle \approx \langle \hat{n}_k \hat{m}_k \rangle \langle (1 - \hat{n}_{k+1})(1 - \hat{m}_{k+1}) \rangle = \Omega_{11}(s_k, q_k) \Omega_{00}(s_{k+1}, q_{k+1})$, where $\Omega_{11}(u, v)$ is given by exact microscopic expression (6). Thus, for a homogeneous state $\langle \hat{n}_k \rangle = u$, $\langle \hat{m}_k \rangle = v$ the meanfield expression gives the exact microscopic stationary current (4). The semiclassical equation of motion becomes

$$\begin{aligned} \frac{\partial s_k}{\partial t} &= +s_{k-1}(1 - q_k) - Q\Omega_{11}(s_{k-1}, q_{k-1})\Omega_{00}(s_k, q_k) \\ &\quad - s_k(1 - q_{k+1}) - Q\Omega_{11}(s_k, q_k)\Omega_{00}(s_{k+1}, q_{k+1}), \end{aligned} \quad (\text{B1})$$

for $k = 2, 3, \dots, N - 1$, complemented with boundary conditions for the boundary sites $k = 1$ and $k = N$

$$s_1(t) = u_L; \quad s_N(t) = u_R; \quad (\text{B2})$$

For left-movers the equations are derived analogously. The complete set of equations of motion can be viewed as a natural discretization scheme with which we integrate numerically the hydrodynamic equations (7). Indeed, by Taylor expansion of (B1), and Euler rescaling of space and time we obtain (7). Comparison with the stochastic evolution shows that both steady state profiles and temporal evolution is described correctly.

-
- [1] T.M. Liggett, *Stochastic interacting systems: contact, voter and exclusion processes* (Springer, Berlin, 1999).
 - [2] G.M. Schütz, in *Phase Transitions and Critical Phenomena*, Vol.19, C.Domb and J.Lebowitz (eds.) (Academic, London, 2001).
 - [3] D. Mukamel, in *Soft and Fragile Matter: Nonequilibrium Dynamics, Metastability and Flow*, Eds. M.E. Cates and M.R. Evans (Institute of Physics Publishing, Bristol, 2000);
 - [4] M. R. Evans and T. Hanney, *J. Phys. A: Math. Theor.* **38** R195 (2005)
 - [5] A. Schadschneider, D. Chowdhury, and K. Nishinari, *Stochastic Transport in Complex Systems* (Elsevier, Amsterdam, 2010)
 - [6] G. M. Schütz, *J. Phys. A* **36**, R339 (2003). *J. Phys. A* **36**, R339 - R379
 - [7] C. Kipnis, C. Landim, *Scaling Limits of Interacting Particle Systems* (Springer, Berlin, 1999).
 - [8] V. Popkov and G. M. Schütz, *Europhys. Lett.* **48**, 257 (1999).
 - [9] V. Popkov, *J. Stat. Mech.* P07003 (2007).
 - [10] V. Popkov and M. Salerno, *Phys. Rev. E* **83**, 011130 (2011).
 - [11] V. Popkov and G. M. Schütz, *Phys. Rev. E* (2012); arXiv:1206.1490
 - [12] G. Q. Chen and P. T. Kan, *Archive for Rational Mechanics and Analysis* **130**, p.326 (1995); *ibid.* **160**, p.325 (2001)
 - [13] P. D. Lax, *Hyperbolic Systems of Conservation Laws and the Mathematical Theory of Shock Waves*, SIAM series, Philadelphia, vol. 11 (1973)
 - [14] P. D. Lax, *Hyperbolic Partial Differential Equations*, Courant Lecture Notes in Mathematics, vol. **14**, AMS, (2006)
 - [15] J. Krug, *Phys. Rev. Lett.* **67**, 1882 (1991)
 - [16] V. Popkov, Infinite reflections of shock fronts in driven diffusive systems with two species, *J. Phys. A* **37**, 1545 - 1557 (2004)
 - [17] G. Schütz and E. Domany, *J. Stat. Phys.* **72**, 277 (1993).
 - [18] B. Derrida, M. R. Evans, V. Hakim, and V. Pasquier, *J. Phys. A* **26**, 1493 (1993).
 - [19] V. Popkov and G. M. Schutz, *J. Stat. Phys.* **112**, 523 (2003).
 - [20] The hydrodynamic limit equations can be obtained by averaging operator equations of motion, as in Appendix B, consequent Taylor expansion $\langle n_{k+1}(t) \rangle \rightarrow u(x + \frac{a}{N}, t) \approx u(x, t) + \frac{a}{N} \partial u / \partial x$, etc., and Euler rescaling of space and time.
 - [21] A stationary rarefaction wave is characterized by the fact it has one zero characteristic velocity ($c_i = 0$),

as opposed to a stationary shock wave where all characteristic velocities are nonzero [13].

- [22] We borrowed the notation from [10].
- [23] M. R. Evans, D. P. Foster, C. Godreche, and D. Mukamel, *Phys. Rev. Lett.* **74** 208 (1995)
- [24] P. F. Arndt, T. Heinzel, and V. Rittenberg, *J. Stat. Phys.* **90**, 783 (1998).
- [25] M. Clincy, M. R. Evans, and D. Mukamel, *J. Phys. A* **34**, 9923 (2001).
- [26] S. Klumpp and R. Lipowsky, *EuroPhys. Lett.* **66** 90 (2005)
- [27] D. W. Erickson, G. Pruessner, B. Schmittmann, and R. K. P. Zia, *J. Phys. A* **38**, L659 (2005).
- [28] R. D. Willmann, G. M. Schütz, and S. Großkinsky, *Europhys. Lett.* **71**, 542 (2005). S. Großkinsky, G. M. Schütz, and R. D. Willmann, *J. Stat. Phys.* **128**, 587 (2007).
- [29] E. Pronina and A. B. Kolomeisky, *J. Phys. A* **40** (2008) 2275
- [30] V. Popkov, M. Evans and D. Mukamel, *J. Phys. A* **41** (2008) 432002
- [31] S. Gupta, D. Mukamel, G.M. Schütz, *J. Phys. A: Math. Theor.* **42**, 485002 (2009).
- [32] Z. D. Sun, R. Jiang, M.-B. Hu and Q.-S. Wu, *Phys.Lett. A* **374** (2010) 4080
- [33] V. Popkov and I. Peschel 2001 *Phys. Rev. E* **64** 026126 (2001).
- [34] V. Popkov, M. E. Fouladvand and G. M. Schütz, *J.Phys. A.* **35**, 7187-7204 (2002).